DEVELOPMENT AND OPTIMIZATION OF TERIFLUNOMIDE-LOADED CHONDROITIN SULPHATE-COATED NANOSTRUCTURED LIPID CARRIERS (NLCS) THROUGH BOX BEHNKEN DESIGN

CRISTÓBAL CAMPOS [1], PABLO TORRES-VERGARA [1], RICARDO GODOY [1], CRISTINA RIQUELME [1], NOEMI ARELLANO-VILLASEÑOR [2], ROCIO ALEJANDRA CHAVEZ-SANTOSCOY [3], ISABEL HERBAS-GOITÍA [1] AND CAROLINA GOMEZ-GAETE [1]*

[1]*Departamento de Farmacia, Facultad de Farmacia, Universidad de Concepción, Chile.*
[2]*Facultad de Ciencias Químicas e Ingeniería, Universidad Autónoma de Baja California-Campus Tijuana, México.*
[3]*Tecnologico de Monterrey, School of Engineering and Science, Monterrey 64849, Mexico*.

Rheumatoid arthritis (RA) is an autoimmune chronic disease characterized by disabling pain and deformity of the joints. Teriflunomide (TFM), a metabolite from leflunomide, is given orally to RA patients, but its gastrointestinal and systemic side effects are severe and not well tolerated. This study aims to optimize and develop nanostructured lipid carriers (NLC) loaded with teriflunomide (NLC-TFM). NLCs were developed by homogenization and ultrasound. The optimization parameters were achieved through a Box-Behnken experimental design. The optimized NLC-TFM were also coated with chondroitin sulfate (NLC-TFM-CHS) to enhance its interaction with target tissues and shift its focus to intra-articular administration. Both formulations were characterized in their morphology, particle size (PS), Zeta potential, entrapment efficiency (EE%), drug loading (DL%), molecular interactions and *in vitro* release kinetics. The developed NLC-TFM and NLC-TFM-CHS exhibited a spherical morphology, Zeta potential lower than -30 mV, mean PS of 178.6-211 nm, EE% of 85.95-65.78 % and DL% of 3.97-2.97%, respectively. Thermal and crystalline behavior analyses suggested that TFM is dissolved within the lipidic matrix. The release of TFM showed a biphasic pattern, with an initial burst release followed by a sustained release, being the latter more marked in NLC-TFM-CHS. The developed formulations show promise as delivery systems for targeted therapy of RA through intra-articular administration.

Keywords: Teriflunomide, rheumatoid arthritis, nanostructured lipid carrier, experiment design.

1. INTRODUCTION

Rheumatoid arthritis (RA) is a systemic autoimmune disease affecting joints, connective tissue, muscles, and tendons.[1] Due to its chronic nature, RA causes incapacitating pain and deformation of joints, but recent research has demonstrated that other organs including lungs, heart, eyes and skin are also affected.[2]

RA treatment mostly aims to slow the disease's progression and severity of its symptoms. Currently, non-steroidal anti-inflammatory drugs (NSAIDs), corticosteroids, and disease-modifying antirheumatic drugs (DMARDs) are regarded as first-line pharmacological therapies. Regarding DMARDs, they are receiving increased interest due to their ability of decreasing or even stopping the damage and deformity of joints, along with a reduction of systemic symptoms [3]

Teriflunomide (TFM), the active metabolite of the DMARD leflunomide, is a drug that inhibits the activity of dihydroorotate dehydrogenase (DHODH), a mitochondrial enzyme overexpressed in proliferating lymphocytes. This inhibition blocks the de novo synthesis of pyrimidines, exerting a cytostatic action over proliferating T- and B-cells and limiting their participation on inflammatory processes involved in the pathogenesis of RA[4]. However, despite their effectiveness in managing the symptoms of RA, the adverse effects profile DHODH inhibitors have been the subject of concerns, since they compromise adherence to treatment [5,6]

In this regard, developing targeted delivery systems based on nanoparticles has become a promising alternative to overcome certain issues associated with RA treatment. Formulations are designed to enhance the permeability of drug in inflamed tissues, reducing the effective dose and the number of administrations over time [7] Over the last decade, several delivery systems based on nanostructured lipid carriers and Solid lipid nanoparticles (SLN) have been developed to treat RA, taking advantage of features including physical stability, biocompatibility, biodegradability, and versatility in the route of administration[7–11]. Furthermore, the hydrophobic nature of NLCs facilitates the encapsulation of hydrophobic drugs such as TFM, and they can be incorporated within hydrogels, microparticles or coated with natural polymers through electrostatic interactions[12–16]. Furthermore, the methodologies employed for the generation of NLCs allow the use of aqueous solvents, being a significant advantage over other techniques that use organic solvents known for their toxicity[17].

Long-term oral use of TEF has systemic complications, such as liver toxicity, alopecia and neutropenia, and GI; such as nausea and diarrhea.[18] Drug-loaded lipid nanoparticles (SLNs and NLCs) can be customized for targeted drug delivery with glycosaminoglycans such as chondroitin sulfate (CHS).[12,19] CHS can actively target affected joints through selective binding to CD44 receptors overexpressed in RA [20]promoting accumulation and retention of the drug in the synovial tissue while minimizing side effects and dosage [21]

Although NLCs have been widely studied as drug delivery systems (DDS), the outcomes associated to the factors involved in their formulation are not always predictable. To address this issue, statistical tools systematize the experimental design and optimize the pre-formulation process, since there is a more detailed analysis of the influence of each factor in the outcome. Among the available experimental designs, the composite central design and Box-Behnken design (BBD) allow the study of more than two levels per factor [22]

In the present study, a CHS-coated NLC encapsulating TFM formulation was prepared through the hot homogenization/ultrasound method under an organic solvent-free environment and optimized through BBD. The impact of formulation factors was assessed in terms of particle size, entrapment efficiency (EE%) and drug loading.

2.- MATERIALS AND METHODS

2.1.- Materials

Compritol 888 ATO was obtained from Gattefossé (Saint Priest, Francia). Lecithin (Soy PC 95%), Glyceryl trioleate (triolein), Pluronic F68 (poloxamer 188) and sodium taurodeoxycholate and Chondroitin sulphate were purchased from Sigma Aldrich (Wisconsin, United States). Teriflunomide, Toronto Research Chemical. (Ontario, Canadá). All the chemicals and solvents were either HPLC or analytical grade. dialysis tubing cellulose membrane (Spectra/Por; 12-14 kDa cut-off, CA, United States).

2.2.- Methods

2.2.1.- Preparation of teriflunomide-loaded nanostructured lipid carrier

The TFM-loaded nanostructured lipid carriers (TFM-NLC) were prepared through the hot homogenization/ultrasound method [23]. Briefly, TFM was added to the lipid phase comprised of Compritol (solid lipid) and triolein (liquid lipid), previously heated at a temperature of 10°C over the fusion point of the

*Corresponding author email: cargomez@udec.cl

solid lipid. Next, the aqueous phase, composed of water, lecithin, sodium taurodeoxycholate and poloxamer 188, was heated to the same temperature of the lipid-TMF mix and added to the latter dropwise. The dispersion was homogenized with an Ultraturrax (Heidolph, Schwabach, Germany) at 20500 RPM for 2 min, and the resulting emulsion was sonicated for 7 min at 80 % amplitude, using a sonicating probe (Vibracell, VCX 130, USA). The nano-dispersion was cooled in an ice bath for 10 min and stored at 4°C. Under the above storage conditions, parameters including particle size and zeta potential were analyzed after one month (see supplementary table 1).

2.2.2.- Experimental design and optimization of formulation parameters

A 3-factor and 3-level Box-Benkhen experiment design was employed for the optimization of formulation parameters. (Design-Expert VR Software Version 10, State-Ease Inc., Minneapolis, MN). A study with 16 experiments was designed (see table 1), analyzing the effect of three factors including: liquid lipid/total lipids ratio (X1), amount of total lipids (X2) and amount of poloxamer 188 (X3), over the responses: particle size (Y1), encapsulation efficiency (%EE) (Y2) and drug loading (DL) (Y3) (Table 2). The desirability function of the Design-Expert VR software was employed to obtain an optimized formulation.

Table 1. *Experimental runs and expected responses defined by the Box-Behnken design.*

Experiment	A: Liquid lipid/ Total lipids	B: Amount of lipid (mg)	C: Amount of surfactant (mg)	Y_1: Particle size (nm)	Y_2: EE (%)	Y_3: DL (%)
1	0.300	500	150	180	90.2	4.58
2	0.200	600	150	227	66.1	2.75
3	0.200	400	300	148	88.4	5.45
4	0.300	600	225	201	91.2	3.79
5	0.100	400	225	151	86.0	5.37
6	0.200	500	225	158	85.7	4.36
7	0.300	500	300	166	88.9	4.47
8	0.100	500	300	167	89.8	4.48
9	0.200	500	225	162	90.6	4.48
10	0.100	500	150	195	77.5	3.90
11	0.200	500	225	187	90.0	4.53
12	0.200	600	300	190	89.7	3.78
13	0.300	400	225	157	91.3	5.76
14	0.200	400	150	168	92.2	5.76
15	0.100	600	225	215	93.4	3.88
16	0.200	500	225	189	88.4	4.19

Table 2. *Independent and dependent variables for the Box-Benkhen experimental design.*

FACTORS	**CODED LEVELS**		
INDEPENDENT VARIABLES	**LOW LEVEL (-1)**	**MEDIUM LEVEL (0)**	**HIGH LEVEL (+1)**
X1: LIQUID LIPID/TOTAL LIPID	0.1	0.2	0.3
X2: TOTAL LIPID (mg)	400	500	600
X3: POLOXAMER 188 (mg)	150	225	300
DEPENDENT VARIABLES	**CONSTRAINTS**		
Y1: PARTICLE SIZE (nm)	=180 nm		
Y2: E.E (%)	MAXIMIZE		
Y3: DRUG LOADING (%)	IN RANGE		

2.2.3.- Coating of NLCs with chondroitin sulfate

The optimized TFM-NLC formulation was coated with CHS. Briefly, TFM-NLCs were prepared as described above, but after sonication, a CHS 1.5% w/v solution was slowly added to the suspension (equivalent to 75 mg of CHS) which corresponds to approximately 15% of the total solid lipids. This amount of CHS was determined according to preliminary experiments. The resulting mixture was homogenized at 8000 RPM for 5 min. The formulation was cooled under a water bath for 10 min and stored at 4°C. Under the above storage conditions, parameters including particle size and zeta potential were analyzed after one month (see supplementary table 1).

2.2.4.- Particle size, polydispersity index and zeta potential

Particle size, polydispersity index and Zeta potential of the prepared formulations were determined with a Malvern Zetasizer Nano-ZS (Malvern, UK), at 25°C with a scattering angle of 90°. The formulations were diluted 100 times with ultrapure water [24]

2.2.5.- Differential scanning calorimetry (DSC)

Differential scanning calorimetry analyses were performed on TFM, Compritol, CHS, physical mixture of TFM and excipients (PHM), NLC-BLANK lyophilizate and NLC-CHS-TFM. Samples were analyzed on a Mettler Toledo DSC instrument model 822e, equipped with high pressure capsules. The heating rate used was 10°C/min in a range of 25-350°C.

2.2.6.- Powder X-ray diffraction (PXRD)

Powder X-ray diffraction analyses were performed for the single drug, solid lipid, coating agent, lyophilized blank NLCs and lyophilized TFM-NLCs, using an Endeavor D4 (Bruker,). Samples were exposed to a Cu radiation and scanned in the range of 2° - 90°, 2θ with a step size of 0.02, at 25°C.

2.2.7.- Atomic force microscopy (AFM)

Morphology of TFM-NLCs and TFM-CHS-NLCs was studied by means of atomic force microscopy (AFM), using a Naio AF microscope (Nanosurf AG, Liestal, Switzerland). The instrument was equipped with a gold-coated PPP-FMAuD tip (Nanosensors®) and samples were analyzed at a resonance frequency of 75 KHz, an elastic constant of 2.8 N/m and 7 nm of radius. Samples were processed by diluting them in ultrapure water (1:1) and deposited onto a plastic substrate, for further dying with N_2 before observation.

2.2.8.- High performance liquid chromatography

The amount of TFM was determined by means of high-performance liquid chromatography (HPLC), using a previously published methodology[25].with adaptations. Samples were analyzed in a LaChrom Elite HPLC system (Merck-Hitachi) equipped with an UV detector set up at 295 nm. Separation of TFM was carried out in a LiChroCart 250 – 4 RP-18 (5 µm) column, using a methanol:phosphate buffer pH 3 (65:35 %v/v), at a flow of 1.0 ml/min. The methodology was validated in terms of linearity, accuracy, precision, limit of detection and limit of quantification according to ICH guidelines [26]

2.2.9.- Encapsulation efficiency and drug loading

The encapsulation efficiency and drug loading of the formulations were calculated according to a previously reported methodology of [27] with modifications. Briefly, a small amount of MeOH was added to 200 mL of TFM-NLC dispersion, and the mixture was centrifuged at 13500 RPM for 25 min. The resulting pellet was filtered through 0.22-µm PVDF filter (Millipore Pvt Ltd.) and the concentration of drug in the supernatant was analyzed with the HPLC methodology previously described. EE% and DL% were calculated with the following equations.

$$\%EE = \left[\frac{WT-WF}{WT}\right] x\ 100 \quad (1)$$

$$\%DL = \left[\frac{WT-WF}{WL}\right] x\ 100 \quad (2)$$

Where WT is the initial weight of TFM, WF is the weight of free TFM, and WL is the weight of total lipids (solid lipids + liquid lipids).

2.2.10.- In vitro drug release kinetics

The release kinetics of TFM from NLCs and CHS-coated NLCs was performed through dialysis[28], under sink conditions. Dialysis membrane (dialysis tubing cellulose membrane, cut-off: 12-14 KDa) was soaked overnight in double distilled water prior to the release studies. A volume of suspension of NLC equivalent to 5 mg of TFM was loaded into a dialysis bag, which afterwards was submerged in 150 mL of medium (0.5% v/v Tween 80 in PBS, pH 7.4). Samples were placed in an oven at 37°C under constant agitation at 100 RPM.[29] The aliquot (500 µL) of medium was withdrawn and replaced with the same volume of PBS at 30 min, 1, 2, 4, 6, 8, 12, 24, 48 and 72 hrs. The amount of TFM released from the NLC was determined via HPLC mentioned previously.

3.- RESULTS AND DISCUSSION

3.1.- Box-Behnken design

The obtained responses in 16 experiments defined by the Box-Benhken design (including four central points) are shown in table 1. The results of the ANOVA performed are presented in table 3.

Table 3. Summary of ANOVA and statistical parameters respective to selected responses indicating significance and fitting of different models.

Parameters of the adjusted model	Particle size: Y_1		Entrapment Efficiency: Y_2		Drug Load: Y_3	
	p-value	Interpretation	p-value	Interpretation	p-value	Interpretation
Model	< 0.0001	Significant	0.0372	Significant	< 0.0001	Significant
R2	0.844	-	0.715	-	0.941	-
Adjusted R2	0.805	-	0.525	-	0.902	-
Predicted R2	0.775	-	-0.305	-	0.730	-
Lack of fit	0.971	Not significant	0.079	Not significant	0.149	No significant
X1	0.425		0.283	Not significant	0.208	No significant
X2	< 0.0001	Significant	0.217	Not significant	< 0.0001	Significant
X3	0.0048	Significant	0.044	Significant	0.127	Not significant
X1X2	-	-	-	-	0.365	Not significant
X2X3	-	-	0.017	Significant	0.207	Not significant
X1X3	-	-	0.178	Not significant	0.028	Significant
$X1^2$	-	-	-	-	-	-
$X2^2$	-	-	-	-	-	-
$X3^2$	-	-	0.102	Not significant	-	-

The obtained responses were analyzed by multiple linear regression using the Design Expert software, which provided fit statistics: coefficient of variation (CV), multiple correlation coefficient (R2), and adjusted multiple correlation coefficient (adjusted R2) (table 3). The comparison of these statistical parameters, using the stepwise method was used to select the mathematical model of best fit (linear, two-way interaction or quadratic) for each dependent variable.

The best fit model for particle size was a linear model, while EE best fit a quadratic model that considers the interaction between X2 and X3. Drug loading was fitted to a 2FI model.

The statistical significance of the fitted models was confirmed by analysis of variance (ANOVA). The terms of the model will be considered significant when Prob>F<0.0500 and not significant Prob>F>0.1000. The interaction of the independent variables (X) and the responses (Y) are observed in three-dimensional (3D) graphs, which also showed their utility in studying the effects of two factors on one response at a time (Figure 1).

3.1.1.- Effects over particle size (Y1)

The linear model selected for particle size gave a R2 value of 0.844 (table 3) which is appropriate since only a 15.6 % of the observed variation in the response is not explained by this model. The resulting equation shows that the variables X2 (lipid amount) and X3 (poloxamer 188 amount) exert significant effects over PS.

$$PS:\ y1 = 179 - 2.98\,x1 + 26.1\,x2 - 12.4\,x3 \quad (3)$$

The prepared formulations exhibited particle sizes in the range of 148 – 227 nm, with an optimal value set up at 180 nm. This choice of PS was established upon the results of preliminary experiments that provided formulations with PS close to 180 nm. Furthermore, a previous report demonstrated in a rodent model of RA that the intravenous administration of TFM-loaded-CHS-coated-nanoliposomes of with a particle size lower than 200 nm tended to accumulate in the synovial region [28]. The effects of X2 (increased PS) and X3 (decreased PS) are consistent with the analysis of variance generated in this study (table 3) and previous reports.[30] In the same trend, the influence of X1 is not significant.[31] A higher amount of solid lipids (X1) increases the average PS due to the availability for the formation of nanoparticles. The negative effects exerted by the surfactant can be explained by the stabilizing effect of poloxamer 188 on the formed droplets, through a reduction of the interfacial tension that favors the reduction in size [32,33].

3.1.2.- Effects over EE%

For EE%, a fitted quadratic model was used. To increase its significance, the model was adjusted, so that the observed R2 value was 0.715 while the adjusted R2 was 0.525 (Table 3). Although R2 is greater than 0.7, the large decrease in adjusted R2 and the negative value of predicted R2 indicate that the mean most likely provides a better response prediction for this parameter.

$$\text{EE\%: } y2 = 89.6 + 1.88x1 - 2.18x2 + 3.84x3 - 3.40x1x3 + 6.83\,x2x3 - 4.23x3^2 \quad (4)$$

The EE% of the obtained formulations varied between 66.1 and 93.4%. The factor X3 (amount of poloxamer 188) and the interaction X2X3 (total lipids and amount of poloxamer 188) exerted a significant and proportional modification of EE%.

As reported in the literature, the increase in the liquid lipid/solid lipid ratio (X1) on EE% has a discrete effect on EE%.[34] As observed in equation 4, the increase in poloxamer 188 exerts a positive effect on EE%, likely due to the increase in the solubility of TFM within the lipid matrix.[35]

The response-surface plot (middle figure 1) shows how the interaction between the surfactant poloxamer 188 and the amount of lipids can significantly increase EE%, as described above (equation 4). If the amount of poloxamer 188 is reduced to a minimum, EE% is markedly decreased. This outcome can be explained by the fact that the molecules of surfactant are not enough to stabilize such amount of lipids. In contrast, if the amount of poloxamer 188 is increased to its maximum and the amount of lipids is reduced to a minimum, EE% also is decreased due to the solubilization of drug in the excess of surfactant instead of the lipid matrix.[36]

3.1.3.- Effects over drug loading

The 2FI model selected provided a R2 value of 0.941 and X2 was the formulation factor that most contributed to DL%, as shown in equation 5. The lack of fit was not significant.

$$\text{DL\% } y3 = 4.47 + 0.121x1 - 1.02\,x2 + 0.151x3 - 0.121x1x2 - 0.172\,x1x3 + 0.332\,x2x3 \quad (5)$$

The amount of total lipids (X2) negatively influences DL% (equation 5). The greater the amount of lipids, the DL% decreases. This could be since to a very wide ratio between the amount of drug and X2 can lead to a deficient saturation of the drug in the lipid matrix and, therefore, a lower availability of the drug within the nucleus of the nanoparticle (Kunal et al., 2015). This outcome may be confirmed in the response-surface plot (bottom figure 1) which shows a more detailed view of interactions between factors.

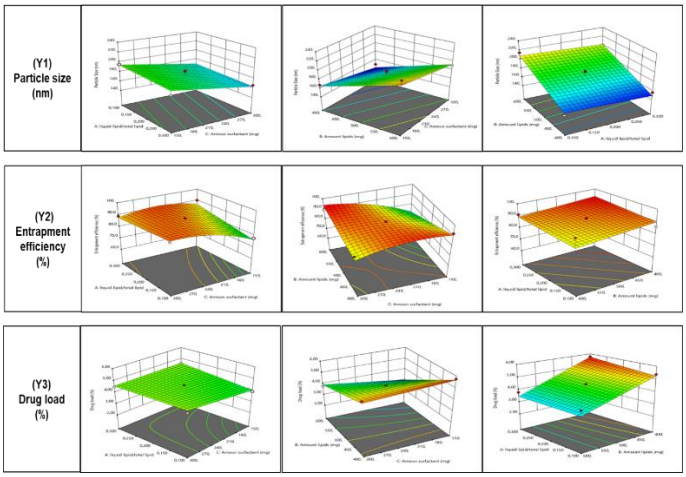

Figure 1. *3D response surface plot for the optimization of the prepared formulations, showing the impact of different formulation variables (independent factors) on the characteristics of the developed NLC;effect of X1, X2 and X3 and their interaction terms on the particle size (Y1);effect of X1, X2 and X3 and their interaction terms on trapping efficiency (Y2); and effect of X1, X2 and X3 and their interaction terms on drug loading (Y3).*

3.2.- Optimization of the developed formulations

The optimization of formulation parameters through the prediction method provides a more accurate choice of values to obtain the desired responses. The design of an optimized NLC-TFM formulation was based on the aim of obtaining a high EE% and DL%, adjusting PS to 180 nm. The resulting formulation has an amount of 539 mg in total lipids, a liquid lipid/total lipid ratio of 0.1 and 297 mg of poloxamer 188. Findings are summarized in table 4.

Table 4. *Particle size (mean diameter), polydispersity index (PDI), zeta potential (ZP), entrapping efficiency (EE%), and drug loading (DL%) of NLCs-TFM and CHS-NLC-TFM (n=3, data are expressed as mean ± SD).*

Formulation	PS (nm)	PDI	ZP (mV)	EE%	DL%
NLC-TFM	178.63 ± 2.49	0.297 ± 0.05	-34.95 ± 1.99	85.95 ± 2.47	3.97 ± 0.01
CHS-NLC-TFM	211.03 ± 0.42	0.248 ± 0.02	-56.35 ± 2.33	65.78 ± 2.54	2.97 ± 0.05

3.3.- Preparation and physicochemical characterization: uncoated-NLCs and chondroitin sulfate coated-NLCs

3.3.1.- Particle size, zeta potential and polydispersity

3.3.1.1.- NLC-TFM

The optimized NLC-TFM formulation exhibited PS, PDI and ZP values of 178.6 ± 2.5 nm, 0.297 ± 0.05 and (-)34.95 ± 0.99 mV, respectively (table 4). Small PS is one of most important features for the effective oral drug delivery of NLCs[37], also it is key for local focalization and retention in joints affected by the disease, since allows NLCs to distribute within the inflamed synovial tissue (~700nm). Furthermore, the distribution and retention of nanoparticles within joints is favored by an initial stage of RA in which the synovial membrane increases the number of cell layers, leading to hypoxia and angiogenesis. As the developed vasculature leaks into the joints, this outcome allows the accumulation of NLCs in the affected zone[38–40]A PDI value close to 0.2 means that the size distribution of NLCs is narrow, improving their performance. Finally, a ZP value close to ± 30 mV reflects better stability of NLCs, due to the repulsion between particles that minimize the formation of aggregates [41,42] .

3.3.1.2.- NLC-TFM-CHS

To improve the colloidal features of NLC-TFM and enhance both active and passive focalization, CHS was added to the formulation [43]. which could favor the intra-articular administration of NLC-TFM[12,19,44]. The sole addition of CHS without the need of organic solvents and chemical reactions, generates a coating of NLC-TFM. The resulting formulation showed a slightly increased PS (table 4), probably due to the external coating with CHS as observed in previous reports [15,28,44] . Although the use of CHS reduced both PDI and ZP as observed in freshly prepared formulations, after one month of storage at 4°C, these parameters and PS were significantly increased. This behavior is suggestive of poor long-term stability and was not observed in the non-coated formulations (see supplementary table 1).

Since the developed NLC-TFM are elaborated with phosphatidylcholine, the coating with CHS is probably mediated by hydrophobic interactions with the former molecule as previously reported [45]. Another study reported an interaction between leflunomide-loaded NLCs and CHS. However, as the developed NLCs in the above study lacked lecithin in their formula, the proposed mechanism was the generation of hydrogen bonding between the carbonyl group of leflunomide and hydroxyl groups of CHS [19]. Since TFM has the same carbonyl group present leflunomide, the interaction with CHS could be similar, so further studies are warranted.

3.4.- Entrapment efficiency and drug loading

The EE% and DL% obtained for NLC-TFM and CHS-NLC-TFM are summarized in table 4. The presented findings suggest that the TFM is properly encapsulated within NLCs, but the addition of CHS has a negative impact on EE%, an effect that can be relatively reduced by adjusting the load of TFM and CHS to find an ideal ratio. This outcome has been previously reported [12,15,21,44] and could be explained by the leaching of TFM from the NLCs, due to the increased time necessary to coat with the CHS solution[46] . Other reported mechanisms are the competitive behavior of TFM and CHS to interact with the hydrophobic sites of lecithin and lipidic components of NLCs.[15] Furthermore, an excess of CHS decreases EE%, probably due to the insufficient amount of surfactant to stabilize both lipids and CHS.

3.3.5.- DSC analysis

The DSC curves of TFM, Compritol, CHS, BLANK-NLC, CHS-NLC-TFM are shown in figure 2. The DSC curve of TFM showed an endothermic peak at 234.18°C, which belongs to the melting point of the drug in its crystalline state (229-233°C)[47]. In the case of Compritol, the endothermic peak at 73.34 °C is also related to its melting point[48], and is still present in both NLC-BLANK y CHS-NLC-TFM, but is less pronounced. Along with the reduction of the above peak, Compritol exhibited a reduction in the onset of the peak from 69 to 63 °C in both formulations. This change in the melting point could be attributed to the decrease in particle size, which increases the specific surface compared to the bulk material (Kelvin effect) [49]. Furthermore, this change could be explained by the interaction between the solid lipids, liquid lipids and surfactants, demonstrating that the NLCs were formed correctly [50].

As bulk material, CHS showed a sharp endothermic peak 197.17°C, related to the polymer's melting point. Both BLANK-NLC y CHS-NLC-TFM present an almost identical curve, except for an endothermic peak at 198°C (corresponding to CHS) in the latter formulation. Finally, CHS-NLC-TFM did not show a peak related to TFM, probably because the drug was dissolved within the lipid matrix during the encapsulation process[51]

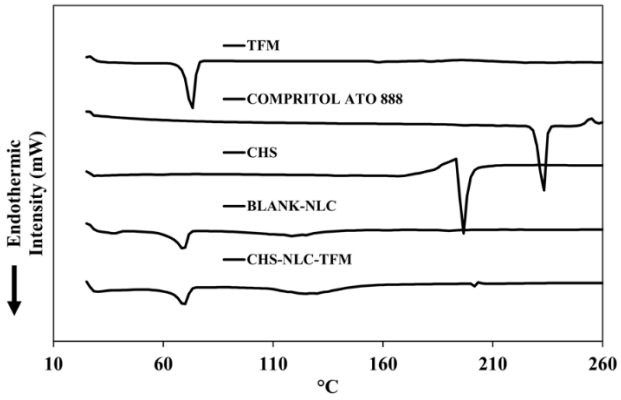

Figure 2. *DSC patterns of drug* ***(TFM)****, solid lipid (****Compritol 888 ATO****), chondroitin sulfate* ***(CHS)****, lyophilized blank NLCs* ***(BLANK-NLC)*** *and lyophilized TFM-loaded CHS-coated NLCs* ***(CHS-NLC-TFM).***

3.3.6.- PXRD analysis

A PXRD analysis was performed in the developed NLCs and their components to investigate changes in the crystallization of lipids, the internal structure of NLCs and how it is affected by the entrapment of TFM. The XRD patterns of TFM, Compritol, CHS, Blank NLCs and CHS-NLC-TFM are shown in figure 3.

The XRD pattern of TFM exhibited sharp peaks at 2θ (7.78°, 12.60°,| 15.63°, 15.96°, 19.34°, 20.17°, 24.68°, etc.), demonstrating its crystalline nature.[52] Regarding Compritol, its XRD pattern showed two characteristic peaks in 2θ 21.09° y 23.32°, which correspond the alpha and beta' polymorphs, respectively[53]

Blank-NLC y CHS-NLC-TFM showed a reduction in the intensity of peaks at 21.09° and 23.32° 2θ , accompanied with an increase in their amplitude, suggestive of changes in the lipid matrix elicited by TFM [54] Furthermore, a small peak was observed at 19.06° 2θ , characteristic of the polymorphic configuration (Bi) of Compritol [55]. The lack of peaks belonging to TFM in the CHS-NLC-TFM patterns (except for a small peak at 29.1° 2θ), suggested that the drug is dissolved within the lipid matrix [54]. The presented findings are in concordance to those observed in the DSC curves, where no TFM peak is observed since the drug changed to its amorphous state or was molecularly solubilized in the lipid phase of NLCs.

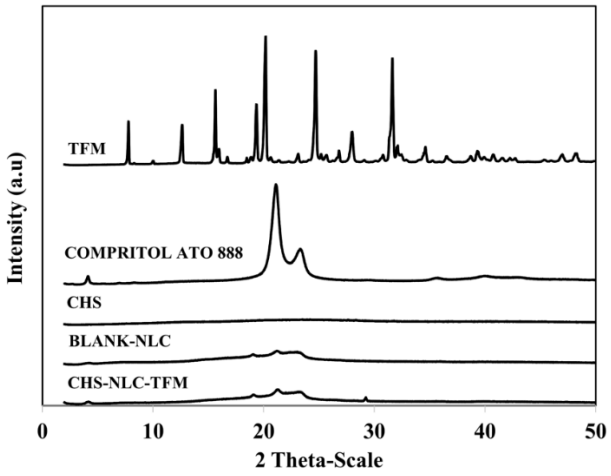

Figure 3. *PXRD patterns of drug* ***(TFM)****, solid lipid (****Compritol 888 ATO)****, chondroitin sulfate* ***(CHS)****, lyophilized blank NLCs* ***(BLANK-NLC)*** *and lyophilized TFM-loaded CHS-coated NLCs* ***(CHS-NLC-TFM).***

3.3.7.- Atomic force microscopy

The observation of the NLC formulations through AFM (Figure 4), showed nanoparticles whose morphology is predominately flat and rounded. However, in the case of NLC-TFM, more aggregation and size heterogeneity were observed compared to the outcome presented by CHS-NLC-TFM. In both formulations TFM crystals were not evidenced in the captured images. The findings are consistent with the presented in the analysis of particle size and PDI carried out by light scattering.

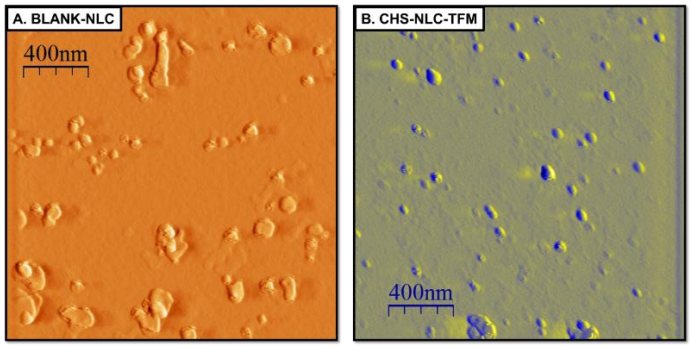

Figure 4. *AFM micrographs of (A) BLANK-NLC and (B) CHS-NLC-TFM.*

3.3.8.- Drug release kinetics

The *in vitro* release kinetics of TFM from the developed formulations are presented in figure 5. The amount of TFM released in NLC-TFM and CHS-NLC-TFM at 72 hours was 40.79 ± 13.44% and 37.68 ± 3.01%, respectively. As observed in other NLC-based formulations elaborated with similar components [51,56,57] the release profile for NLC-TFM is biphasic, with a burst effect that released approximately 30% of TFM within the 4 first hours, followed by a sustained release until 72 h. In the case of CHS-NLC-TFM, the release of drug is slower than the observed on NLC-TFM, suggesting the ability of CHS to form an outer layer capable of retaining the TFM located at the surface of the NLC. This feature has been evidenced in previous studies [21]

In comparison to other nanoparticulated release systems including NLCs loaded with TFM, our formulations show a slightly more sustained release of the drug over time[28,58,59]. The release of TFM as free drug was fast, reaching a 98.45% in 12 h. In contrast, the sustained release of TFM after 12 h could be attributed to the phospholipid/Compritol lipidic barrier,[24] which restricts the penetration of aqueous medium into the Compritol-lecithin-triolein core and reduces the mobilization of TFM, prolonging its release over time [48]

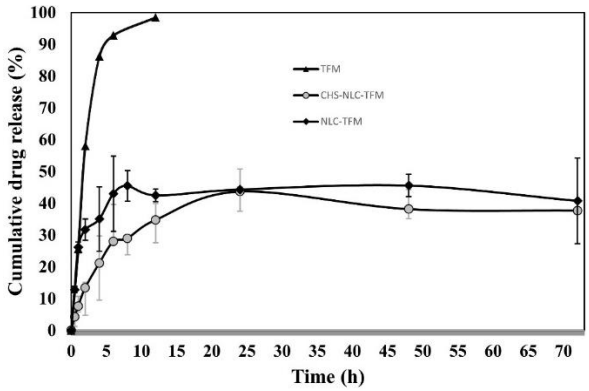

Figure 5. *In vitro release of TFM as free drug, from optimized NLC-TFM and CHS-NLC-TFM. Results are presented as mean ± SD of two independent experiments*

Lipid-based nanocarriers have been shown to significantly improve the efficacy of DMARDs in experimental models of RA.[60] Furthermore, NLCs have favorable biopharmaceutical characteristics, such as better biocompatibility and biodegradability, compared to the classical polymeric materials used.[61]

In the case of CHS-NLC-TFN, this formulation may work as a drug delivery system for the intra-articular route due to the increase in concentration and retention time at the affected joint[12,15,44]. These effects can be enhanced by combining NLCs with other vehicles including hydrogels or hybrid microparticles [8].

CONCLUSIONS

In this work, we showed the development of a specialized formulation for the delivery of TFM, employing a simple methodology that avoids using organic solvents. However, apart from its simplicity, we took advantage of this feature to optimize the formulation parameters that determine the outcome. Experimental designs are widely employed in pharmaceutical development, but we provide first evidence of its use on nanostructured lipid carriers loaded with TFM.

The optimized NLC-TFM formulation was satisfactory regarding its morphological and physicochemical characterization. As the coating with CHS exerted a detrimental effect on EE %, further studies will test the effect of other biocompatible coatings on the properties of NLC-TFM for intraarticular administration.

In conclusion, the development of NLC-TFM and optimization of its formulation parameters results in a product with optimal characteristics for its testing in biological models of inflammation prior to potential use as an intraarticular delivery system.

ACKNOWLEDGEMENTS

The authors would like to acknowledge the support from VRID 219.074.063-INV, Universidad de Concepción.

DISCLOSURE

The authors report no conflict of interests.

ABBREVIATIONS

RA: rheumatoid arthritis, DMDARDs: disease-modifying antirheumatic drugs, TFM: teriflunomide, CHS: Chondroitin sulphate, SLN: Solid lipid nanoparticles, NLC: Nanostructured lipid Carriers, NSAIDs: nonsteroidal anti-inflammatory drugs, DL: drug loading, BBD: Box-Behnken design, PS: particle size, PDI: polydispersity index, EE: entrapment efficiency, DSC: differential scanning calorimetry, PXRD: powder X-ray diffraction, DHODH: dihydroorotate dehydrogenase, TFM-NLC: TFM-loaded nanostructured lipid carriers. DDS: Drug Delivery System, HPLC: high-performance liquid chromatography.

REFERENCES

1. Aletaha, D.; Smolen, J. S. JAMA - Journal of the American Medical Association 2018, 320, 1360–1372. doi:10.1001/jama.2018.13103
2. Conforti, A.; Di Cola, I.; Pavlych, V.; Ruscitti, P.; Berardicurti, O.; Ursini, F.; Giacomelli, R.; Cipriani, P. Autoimmun Rev 2021, 20, 102735. doi:10.1016/j.autrev.2020.102735
3. Scherer, H. U.; Häupl, T.; Burmester, G. R. The Etiology of Rheumatoid Arthritis. Journal of Autoimmunity. Academic Press June 1, 2020, p 102400. doi:10.1016/j.jaut.2019.102400
4. Bar-Or, A.; Pachner, A.; Menguy-Vacheron, F.; Kaplan, J.; Wiendl, H. Drugs 2014, 74, 659. doi:10.1007/S40265-014-0212-X
5. Muehler, A.; Kohlhof, H.; Groeppel, M.; Vitt, D. Drugs in R and D 2019, 19, 351–366. doi:10.1007/s40268-019-00286-z
6. Fragoso, Y. D.; Brooks, J. B. B. Expert Rev Clin Pharmacol 2015, 8, 315–320. doi:10.1586/17512433.2015.1019343
7. Sharma, M.; Chaudhary, D. Int J Pharm 2021, 594, 120176. doi:10.1016/j.ijpharm.2020.120176
8. Shinde, C. G.; Pramod Kumar, T. M.; Venkatesh, M. P.; Rajesh, K. S.; Srivastava, A.; Osmani, R. A. M.; Sonawane, Y. H. RSC Adv 2016, 6, 12913–12923. doi:10.1039/c5ra22672d
9. Garg, N. K.; Tandel, N.; Bhadada, S. K.; Tyagi, R. K. Front Pharmacol 2021, 12, 2194. doi:10.3389/FPHAR.2021.713616/BIBTEX
10. Ye, J.; Wang, Q.; Zhou, X.; Zhang, N. Int J Pharm 2008, 352, 273–279. doi:10.1016/j.ijpharm.2007.10.014
11. Syed, A.; Devi, V. K. J Drug Deliv Sci Technol 2019, 53, 101217. doi:10.1016/j.jddst.2019.101217
12. Bishnoi, M.; Jain, A.; Hurkat, P.; Jain, S. K. J Drug Target 2014, 22, 805–812. doi:10.3109/1061186X.2014.928714
13. Rabelo, R. S.; Oliveira, I. F.; da Silva, V. M.; Prata, A. S.; Hubinger, M. D. Int J Biol Macromol 2018, 119, 902–912. doi:10.1016/J.IJBIOMAC.2018.07.174
14. Zhou, M.; Hou, J.; Zhong, Z.; Hao, N.; Lin, Y.; Li, C. Drug Deliv 2018, 25, 716–722. doi:10.1080/10717544.2018.1447050
15. Jain, A.; Mishra, S. K.; Vuddanda, P. R.; Singh, S. K.; Singh, R.; Singh, S. Nanomedicine 2014, 10, e1031–e1040. doi:10.1016/j.nano.2014.01.008
16. Zewail, M.; Nafee, N.; Helmy, M. W.; Boraie, N. Drug Delivery and Translational Research 2021 2021, 1–24. doi:10.1007/S13346-021-00992-9
17. Akbari, J.; Saeedi, M.; Ahmadi, F.; Hashemi, S. M. H.; Babaei, A.; Yaddollahi, S.; Rostamkalaei, S. S.; Asare-Addo, K.; Nokhodchi, A. Pharm Dev Technol 2022, 1–53. doi:10.1080/10837450.2022.2084554
18. Wiese, M. D.; Rowland, A.; Polasek, T. M.; Sorich, M. J.; O'Doherty, C. Expert Opin Drug Metab Toxicol 2013, 1025–1035. doi:10.1517/17425255.2014.894019
19. Zewail, M.; Nafee, N.; Helmy, M. W.; Boraie, N. Int J Pharm 2019, 567, 118447. doi:10.1016/j.ijpharm.2019.118447
20. Zhao, L.; Liu, M.; Wang, J.; Zhai, G. Chondroitin Sulfate-Based Nanocarriers for Drug/Gene Delivery. Carbohydrate Polymers. Elsevier Ltd July 30, 2015, pp 391–399. doi:10.1016/j.carbpol.2015.07.063
21. Shilpi, S.; Upadhaye, S.; Shivvedi, R.; Gurnany, E.; Chimaniya, P.; Singh, A.; Chouhan, M.; Khatri, K. Asian J Pharm Pharmacol 2019, 5, 495–502. doi:10.31024/ajpp.2019.5.3.10
22. Scioli Montoto, S.; Muraca, G.; Ruiz, M. E. Front Mol Biosci 2020, 7. doi:10.3389/fmolb.2020.587997
23. Nnamani, P. O.; Hansen, S.; Windbergs, M.; Lehr, C. M. Int J Pharm 2014, 477, 208–217. doi:10.1016/j.ijpharm.2014.10.004
24. Rudhrabatla, V. S. A. P.; Sudhakar, B.; Reddy, K. V. N. S. BioNanoScience 2019 10:1 2019, 10, 168–190. doi:10.1007/S12668-019-00680-6
25. Van Roon, E. N.; Yska, J. P.; Raemaekers, J.; Jansen, T. L. T. A.; Van Wanrooy, M.; Brouwers, J. R. B. J. J Pharm Biomed Anal 2004, 36, 17–22. doi:10.1016/j.jpba.2004.05.019
26. ICH Expert Working Group. STABILITY TESTING OF NEW DRUG SUBSTANCES AND PRODUCTS Q1A(R2). In International Journal of Pharmaceutical Sciences Review and Research; 2003; Vol. 2, p 18. doi:10.1136/bmj.333.7574.873-a
27. Pandian, S. R. K.; Pavadai, P.; Vellaisamy, S.; Ravishankar, V.; Palanisamy, P.; Sundar, L. M.; Chandramohan, V.; Sankaranarayanan, M.; Panneerselvam, T.; Kunjiappan, S. Naunyn Schmiedebergs Arch Pharmacol 2020. doi:10.1007/s00210-020-02015-9
28. Mahtab, A.; Rabbani, S. A.; Neupane, Y. R.; Pandey, S.; Ahmad, A.; Khan, M. A.; Gupta, N.; Madaan, A.; Jaggi, M.; Sandal, N.; Rawat, H.; Aqil, M.; Talegaonkar, S. Carbohydr Polym 2020, 250, 116926. doi:10.1016/j.carbpol.2020.116926
29. Elmowafy, M.; Shalaby, K.; Badran, M. M.; Ali, H. M.; Abdel-Bakky, M. S.; Ibrahim, H. M. Int J Pharm 2018, 550, 359–371. doi:10.1016/J.IJPHARM.2018.08.062
30. Martins, S.; Tho, I.; Souto, E.; Ferreira, D.; Brandl, M. European Journal of Pharmaceutical Sciences 2012, 45, 613–623. doi:10.1016/j.ejps.2011.12.015
31. Gordillo-Galeano, A.; Mora-Huertas, C. E. European Journal of Pharmaceutics and Biopharmaceutics 2018, 133, 285–308. doi:10.1016/j.ejpb.2018.10.017
32. Aslam, M.; Aqil, M.; Ahad, A.; Najmi, A. K.; Sultana, Y.; Ali, A. J Mol Liq 2016, 219, 897–908. doi:10.1016/J.MOLLIQ.2016.03.069
33. Kim, M.-H.; Kim, K.-T.; Sohn, S.-Y.; Lee, J.-Y.; Lee, C. H.; Yang, H.; Lee, B. K.; Lee, K. W.; Kim, D.-D. Int J Nanomedicine 2019, 14, 8509. doi:10.2147/IJN.S215835
34. Salvi, V. R.; Pawar, P. J Drug Deliv Sci Technol 2019, 51, 255–267. doi:10.1016/J.JDDST.2019.02.017
35. Raina, H.; Kaur, S.; Jindal, A. B. J Drug Deliv Sci Technol 2017, 39, 180–191. doi:10.1016/j.jddst.2017.02.013
36. Kiss, E. L.; Berkó, S.; Gácsi, A.; Kovács, A.; Katona, G.; Soós, J.; Csányi, E.; Gróf, I.; Harazin, A.; Deli, M. A.; Budai-Szűcs, M. Pharmaceutics 2019, 11. doi:10.3390/PHARMACEUTICS11120679
37. Soni, K.; Rizwanullah, Md.; Kohli, K. https://doi.org/10.1080/21691401.2017.1408124 2017, 46, 15–31. doi:10.1080/21691401.2017.1408124
38. Emami, J.; Ansarypour, Z. Res Pharm Sci 2019, 14, 471–487. doi:10.4103/1735-5362.272534
39. Liu, L.; Guo, W.; Liang, X.-J. Biotechnol J 2019, 14, 1800024. doi:10.1002/biot.201800024
40. Wang, Q.; Sun, X. Biomater Sci 2017, 5, 1407–1420. doi:10.1039/c7bm00254h
41. Bashiri, S.; Ghanbarzadeh, B.; Ayaseh, A.; Dehghannya, J.; Ehsani, A. LWT 2020, 119, 108836. doi:10.1016/J.LWT.2019.108836
42. Trujillo, C. C.; Wright, A. J. J Am Oil Chem Soc 2010, 87, 165–196. doi:10.1039/9781847550842-00103
43. Pirmardvand Chegini, S.; Varshosaz, J.; Taymouri, S. Artif Cells Nanomed Biotechnol 2018, 46, 502–514. doi:10.1080/21691401.2018.1460373
44. Ebada, H. M. K.; Nasra, M. M. A.; Nassra, R. A.; Abdallah, O. Y. Drug Deliv 2022, 29, 652–663. doi:10.1080/10717544.2022.2041130
45. Da Silva, I. M.; Boelter, J. F.; Da Silveira, N. P.; Brandelli, A. Journal of Nanoparticle Research 2014, 16, 1–10. doi:10.1007/s11051-014-2479-y
46. Sharma, A.; Baldi, A. J Dev Drugs 2018. doi:10.4172/2329-6631.1000191
47. Mahtab, A.; Rizwanullah, M.; Pandey, S.; Leekha, A.; Rabbani, S. A.; Verma, A. K.; Aqil, M.; Talegaonkar, S. J Drug Deliv Sci Technol 2019, 51, 383–396. doi:10.1016/j.jddst.2019.03.008
48. Kar, N.; Chakraborty, S.; De, A. K.; Ghosh, S.; Bera, T. European Journal of Pharmaceutical Sciences 2017, 104, 196–211. doi:10.1016/j.ejps.2017.03.046
49. Shah, B.; Khunt, D.; Bhatt, H.; Misra, M.; Padh, H. J Drug Deliv Sci Technol 2016, 33, 37–50. doi:10.1016/j.jddst.2016.03.008
50. Khan, S.; Shaharyar, M.; Fazil, M.; Baboota, S.; Ali, J. European Journal of Pharmaceutics and Biopharmaceutics 2016, 108, 277–288. doi:10.1016/j.ejpb.2016.07.017
51. Zewail, M.; EL-Deeb, N. M.; Mousa, M. R.; Abbas, H. Int J Pharm 2022, 623. doi:10.1016/j.ijpharm.2022.121939
52. Gadhave, D.; Rasal, N.; Sonawane, R.; Sekar, M.; Kokare, C. Int J Biol Macromol 2021, 167, 906–920. doi:10.1016/J.IJBIOMAC.2020.11.047

53. Jenning, V.; Thünemann, A. F.; Gohla, S. H. Int J Pharm 2000, 199, 167–177. doi:10.1016/S0378-5173(00)00378-1
54. Almeida, O. P.; de Freitas Marques, M. B.; de Oliveira, J. P.; da Costa, J. M. G.; Rodrigues, A. P.; Yoshida, M. I.; Mussel, W. da N.; Carneiro, G. J Food Sci Technol 2022, 59, 805–814. doi:10.1007/s13197-021-05078-5
55. Castro, G. A.; Ferreira, L. A. M.; Oréfice, R. L.; Buono, V. T. L. Powder Diffr 2008, 23, S30–S35. doi:10.1154/1.2903515
56. Pinheiro, M.; Ribeiro, R.; Vieira, A.; Andrade, F.; Reis, S. Drug Des Devel Ther 2016, 10, 2467–2475. doi:10.2147/DDDT.S104395
57. Das, S.; Ghosh, S.; De, A. K.; Bera, T. Int J Biol Macromol 2017, 102, 996–1008. doi:10.1016/j.ijbiomac.2017.04.098
58. Gadhave, D. G.; Kokare, C. R. Drug Dev Ind Pharm 2019, 45, 839–851. doi:10.1080/03639045.2019.1576724
59. Pandey, S.; Kumar, V.; Leekha, A.; Rai, N.; Ahmad, F. J.; Verma, A. K.; Talegaonkar, S. Pharm Res 2018, 35, 1–17. doi:10.1007/s11095-018-2478-2
60. Chuang, S. Y.; Lin, C. H.; Huang, T. H.; Fang, J. Y. Nanomaterials 2018, 8, 42. doi:10.3390/nano8010042
61. H. Muller, R.; Shegokar, R.; M. Keck, C. Curr Drug Discov Technol 2011, 8, 207–227. doi:10.2174/157016311796799062